

Enhancement of J_c by Hf -Doping in the Superconductor MgB_2 : A Hyperfine Interaction Study

A.Talapatra¹, S.K.Das¹, S.K.Bandyopadhyay^{1*}, P.Barat¹, Pintu Sen¹, R.Rawat²,
A.Banerjee², T. Butz³

1.Variable Energy Cyclotron Centre, 1/AF, Bidhan Nagar, Kolkata-700 064, India.

2.UGC-DAE Consortium for Scientific Research, Khandwa Road, Indore, 452 017.

3. Universität Leipzig, Fakultät für Physik und Geowissenschaften, Institut für
Experimentelle Physik II, Linnéstraße 5, 04103 Leipzig, Germany

Abstract:

Measurements of the critical current density (J_c) by magnetization and the upper critical field (H_{c2}) by magnetoresistance have been performed for hafnium-doped MgB_2 . There has been a remarkable enhancement of J_c as compared to that by ion irradiation without any appreciable decrease in T_c , which is beneficial from the point of view of applications. The irreversibility line extracted from J_c shows an upward shift. In addition, there has been an increase in the upper critical field which indicates that Hf partially substitutes for Mg. Hyperfine interaction parameters obtained from time differential perturbed angular correlation (TDPAC) measurements revealed the formation of HfB and HfB₂ phases along with the substitution of Hf. A possible explanation is given for the role of these species in the enhancement of J_c in MgB_2 superconductor.

PACS No. 61.66Fn, 74.70.-b, 74.72.-h

Keywords: A. Superconductors; C. X-ray Diffraction; D. Superconductivity;

*Corresponding author; e-mail: skband@veccal.ernet.in

Introduction:

Disorder in type II superconductors plays important roles like pinning the magnetic flux lines in the mixed phase. Pinning of these flux lines increases the critical current density (J_c) and irreversibility field [$H_{irr}(T)$]. With the introduction of disorder, there are changes in both microscopic and macroscopic properties. Disorder and defects in the superconducting materials alter the thermodynamic properties like the upper critical field (H_{c2}) and the coherence length (ξ). Different methods are used to enhance J_c and thermodynamic properties like defect creation by ion irradiation, grain refinement, element doping etc. We had earlier studied J_c and H_{c2} of bulk polycrystalline MgB_2 irradiated with Ne ions. There was an enhancement of H_{c2} , but the change in J_c was marginal [1]. An alternate way to introduce defects is by introducing impurity atoms of different valence states than the host ions. There are reports of Ti and Zr doping in MgB_2 [2]. These group IV elements on Mg^{+2} substitutional site for example introduce additional charge (+2) in the cation site. It is highly probable that dopants go either to Mg site or to B site and cause an enhancement of H_{c2} . However, it is not clearly known whether the dopants are substituted at Mg or B positions. Hence it would be very important to have an idea of the site occupancies of the dopant to specify the roles of different species in the enhancement of J_c , H_{irr} and H_{c2} . Hyperfine interaction techniques like time differential perturbed angular correlation (TDPAC) offer a great potential to understand the nature of sites occupied by the dopant which should be a nuclear probe for this technique. This technique has atomic scale resolution and is extremely sensitive to trace quantities of probe atoms. TDPAC essentially measures the hyperfine parameters, i.e. the electric field gradient (EFG) and asymmetry parameter η . Both these parameters

are sensitive to the electron distribution around the probe nucleus. The measurement of the EFG thus can help telling us the kind of the site the probe is occupying. In other words, it identifies the species formed by the probe atom. In this paper, we have analysed the change in the upper critical field (H_{c2}), J_c and H_{irr} of Hf-doped MgB_2 as compared to the undoped one. We provide here the plausible reasons for the enhancement of H_{c2} and J_c by interpreting the parameters from TDPAC and X-ray diffraction (XRD) measurements. ^{181}Hf , which can be obtained by neutron irradiation of the Hf-doped MgB_2 , is the nuclear probe for the TDPAC measurement in this work. We have employed only 1% Hf, as it is difficult to introduce dopant in higher concentration without causing a severe reduction in T_c , since MgB_2 with its unique structure is extremely sensitive to solid solubility of other ions with different atomic size and valency [3]. As a reference material, we have employed Hf-boride synthesised under identical conditions to that of Hf-doped MgB_2 . This was done to identify any HfB_x species formed in the Hf-doped MgB_2 .

Experimental:

Hf-doped MgB_2 and HfB_x bulk samples were prepared using solid-state reaction. Mg and B powders were taken stoichiometrically with 1 atomic percent of Hf powder. They were mixed thoroughly and pelletized. The pellets were wrapped in a Ta foil and put in a quartz tube which was then evacuated and sealed in He atmosphere and put in a furnace preheated at 1073K and heated for two hours and then at 1173K for another two hours [4]. The tube was then furnace cooled. The samples were characterized by XRD taken on a Philips PW 1710 diffractometer with $\text{Cu } K_\alpha$ of wavelength 1.54Å. The resistivity and T_c of the samples were measured using the four-probe technique [4]. The

same procedure was followed for the case of HfB_x except that the temperatures employed were 1173K and 1373K to check the extent of formation of other compounds of Hf and B like HfB or HfB_2 .

H_{c2} was obtained from magnetoresistance measurements of samples in a Philips 8T cryostat. The magnetisation measurements were carried out at 14 T QD PPMS VSM at different temperatures.

Hf-doped MgB_2 and HfB_x were neutron activated to produce ^{181}Hf which decays to ^{181}Ta in the samples. These samples were annealed at 1173K after irradiation for 4 hours to remove any defect introduced by the neutron activation and counted for the coincidence of the 131-482 keV cascade of ^{181}Hf using a TDPAC camera [5] consisting of six BaF_2 detectors coupled to a fast-slow coincidence set up.

Results and Discussions:

Figs. 1(a, b) show the XRD patterns of Hf doped MgB_2 annealed at 1173K and HfB_x annealed at 1173K. The XRD pattern in Fig. 1a clearly reveals the similarity to pure MgB_2 . It might be due to the fact that at the level of doping employed (1%), the formation of phases containing Hf-boride or substitution of Hf in B or Mg sites is not detectable by XRD. Fig. 1b reflects the formation of multiphase HfB_x with the peaks being indexed with the reflection planes corresponding to both HfB and HfB_2 . Thus, it may be surmised that, at the temperature of formation (1173K) for Hf-doped MgB_2 (temperature needed for the formation of MgB_2), there is a mixture of HfB and HfB_2 .

The transition temperatures $T_c^{(R=0)}$ of undoped and doped samples are 38.0K and 36.4K respectively, with transition widths (ΔT_c) of 0.5K and 1.9K, respectively, as displayed in Fig. 2. Thus, $T_c^{(\text{onset})}$ for the undoped sample is 38.5K and that of the doped

sample is 38.3K. There is little change in $T_c^{(\text{onset})}$ due to 1% Hf doping. However, here is an increase in resistivity and ΔT_c of the doped sample. The residual resistivity of the undoped sample as obtained by extrapolation is $19.0 \mu\Omega\text{-cm}$ and that of the doped sample is $78.8 \mu\Omega\text{-cm}$. The doping in MgB_2 generally causes a decrease in T_c and increase in resistivity [6-8] excepting for the MgO addition where there is an enhancement of T_c [9].

MgB_2 is a multiband superconductor. It has four bands at the Fermi surface (E_F). Two of them, σ -bands (bonding and antibonding) are formed mainly by the p_x+p_y electrons of boron and the other two π -bands (bonding and antibonding) formed mainly by p_z electrons of boron. The origin of superconductivity lies in the σ -bands. These bands are not saturated and the hole on the top of σ -band couples with E_{2g} phonons to give rise to superconductivity. These bands are two dimensional (2D) in character while the π -bands are three dimensional (3D). T_c of MgB_2 is closely proportional to the density of states of σ -bands [10]. Kortus et al. found that the T_c drop is associated to band filling and interband scattering [11].

Fig. 3 shows the upper critical fields of the samples. There is an increase in H_{c2} due to Hf-doping. We have fitted the $H_{c2}(T)$ curve with phenomenological equation:

$$H_{c2}(T) = H_{c2}(0) \left\{ 1 - \left(\frac{T}{T_c} \right)^2 \right\}^\alpha \quad (1)$$

This gives $H_{c2}(0)$ as 18.7 T and 24.2 T for undoped and Hf doped MgB_2 respectively. The enhancement is quite large as compared to that by Neon irradiation [1]. The increase in H_{c2} in the doped sample is due to Hf doping. Enhancement of H_{c2} was observed by Braccini et al. [12] by carbon doping and He ion irradiation on MgB_2 and they explained

the enhancement by disorder introduced through doping. In multiband MgB₂, there is no correlation between the enhancement of H_{c2} and the resistivity change due to doping or ion irradiation [13]. Superconducting parameters like H_{c2} and T_c are governed by coupling of carriers in the 2D σ-band [14], whereas conductivity is primarily controlled by the scattering in the 3D π-band [13]. The appreciable increase in H_{c2} is indicative of some substitution of Hf in Mg or B sites. But, substitution in B site is likely to cause a damage to the coupling of carriers in the 2D σ-band and hence a drastic decrease in T_c^(onset) which is absent here. Hf, if at all, is likely to be substituted dominantly in Mg site which affects the scattering in the 3D π-band and, hence the conductivity. The increase in resistivity of the doped sample is an indication of Hf substitution in Mg site as well as a decrease in grain connectivity [15]. The temperature dependence of H_{c2}(T) is described well by a theory of dirty two-gap superconductivity.

The critical current density J_c was obtained using Bean's critical state model:

$$J_c = \frac{20 \Delta M}{V a \left(1 - \frac{a}{3b}\right)} \quad (2)$$

$\Delta M = (M_+ - M_-)$, where M_± is the magnetic moment obtained from isothermal magnetisation measurements. The measurements were carried out at different fields. *a* and *b* are widths of the samples. *V* is the volume of the samples. The measurements were also carried out at different temperatures. Figs. 4a and 4b show the variations of J_c of both pristine and Hf-doped MgB₂ at 2K and 20K. In both cases, the enhancements of J_c for Hf doped MgB₂ are quite large as compared to that by Ne irradiation [1]. At the same time, the decrease of J_c with applied magnetic field is lower than the undoped sample.

The irreversibility fields (H_{irr}) for the samples were obtained using the criteria that it is that field where the critical current density, $J_c = 100 \text{ A/cm}^2$. The irreversibility lines (IL) of the samples are shown in the inset of Fig. 3. There is an upward shift in the IL in case of the doped sample. The IL was found to scale with temperature in the same way as H_{c2} . $H_{irr}(0)$ for the undoped and doped samples were obtained as 9T and 13.4T, respectively. Thus doping with Hf also improved the irreversibility field.

In the MgB_2 system, J_c and H_{irr} are net outcomes of grain connectivity and flux pinning induced by grain boundaries and precipitates. In Ne-ion irradiated MgB_2 samples, we noticed that though there was no appreciable decrease in T_c , the resistivity increased and J_c decreased due to the reduction in grain connectivity [15] without appreciable change in $T_c^{(R=0)}$. On the contrary, Hf-doped MgB_2 shows a substantial increase in J_c with little change in $T_c^{(\text{onset})}$. The change in $T_c^{(R=0)}$ is due to the increase in transition width ΔT_c . In Hf-doped MgB_2 , the higher J_c may be due to Hf substitution on Mg site (as it is not very likely to go to B-site) and pinning centres formed by precipitation of HfB and HfB_2 which are likely to accumulate in the grain boundary. The grain boundary pinning is the dominant picture in MgB_2 . The pinning force density $F_p (= J_c \times B)$ at different temperatures for both samples are shown in Fig. 5. At lower temperatures, F_p of the doped sample is higher compared to the undoped sample. It was seen by Dou et al. [16] that SiC precipitation in MgB_2 causes an enhancement of J_c . In SiC nanoparticle doping into MgB_2 , it is explained that C-substitution in B sites deteriorates the crystallinity of MgB_2 grains resulting in an enhancement of grain boundary pinning [17, 18]. Analyses based on the grain boundary pinning theory revealed that the origin of J_c enhancement comes from the increase of grain boundary density due

to the suppression of grain growth and as well as an enhancement of f_{gB} (grain boundary pinning force) due to the existence of non-superconducting phases [19] like HfB and HfB₂ in this case. The idea or estimate of these phases as well as the occupancy of Hf at various sites were obtained from TDPAC analysis as is described below.

TDPAC Analysis:

The nuclear interaction of the I=5/2 intermediate state in ¹⁸¹Ta leads to a splitting with three eigenvalues, E₁, E₂ and E₃ : [20]

$$E_1 = -2r \cos\left(\frac{\varphi}{3}\right)$$

$$E_2 = r \cos\left(\frac{\varphi}{3}\right) - \sqrt{3} r \sin\left(\frac{\varphi}{3}\right)$$

$$E_3 = r \cos\left(\frac{\varphi}{3}\right) + \sqrt{3} r \sin\left(\frac{\varphi}{3}\right)$$

With $\cos\varphi = q/r^3$

$$r = \text{sign}(q)\sqrt{|p|}$$

$$p = -28(1 + \eta^2/3)$$

$$q = -80(1 - \eta^2)$$

with the asymmetry parameter η of the electric field gradient defined as $\eta = (V_{xx} - V_{yy})/V_{zz}$.

The three precession frequencies are:

$$\omega_1 = (E_2 - E_3)\omega_Q$$

$$\omega_2 = (E_1 - E_2)\omega_Q$$

$$\omega_3 = (E_1 - E_3)\omega_Q$$

with the quadrupole frequency :

$$\omega_Q = \frac{eQV_{zz}}{40\hbar}$$

where Q denotes the quadrupole moment of the $I = 5/2$ state and V_{zz} is the largest component by magnitude of the EFG tensor. The perturbation function is thus:

$$G_2(t) = a_0 + a_1 \cos \omega_1 t + a_2 \cos \omega_2 t + a_3 \cos \omega_3 t$$

The experimental data were fitted with this function modified using finite distributions of ω_Q . In the present case we have used Lorentzian distributions.

Fig.6 shows the TDPAC spectrum for the Hf-doped MgB_2 sample annealed at 1173K. The perturbation function is shown on the left and the corresponding cosine transform on the right. The results of the least square fit of the data are presented in Table-1. There are four frequencies corresponding to four inequivalent sites where Hf is present in MgB_2 sample. To identify the sites occupied or the species formed by Hf, the TDPAC study was carried out for a sample of HfB_x prepared under identical conditions as that of MgB_2 . Fig. 7 shows the TDPAC spectra for HfB_x annealed at 1173K and 1373K. The results obtained from these spectra are presented in Table-2. At both temperatures, the spectrum for HfB_x could be fitted with two frequencies, which indicates that Hf exists in two inequivalent sites in HfB_x . A closer look at Table-2 indicates that site-II can be assigned to HfB_2 for which our experimental quadrupole frequency agrees with the literature value [21]. From the symmetry of HfB_2 (P/6mmm) the asymmetry parameter η is expected to be zero. The apparent nonzero η is most likely related to the finite linewidth (or finite δ).

The identification of the site-I is not obvious. However, the comparison with XRD results indicates that this low frequency component is most probably the hafnium monoboride, HfB. The site occupancy of this frequency reduces and that of site-II increases with temperature, indicating the conversion of this species to HfB₂. The large δ of this site compared to HfB₂ indicates that this species is nonstoichiometric in nature or there could be partial amorphisation if larger islands are formed. HfB is kinetically stable whereas HfB₂ is thermodynamically stable. That is why at the low reaction temperature of 1173K, a considerable amount of HfB is formed along with HfB₂, but at the higher temperature of 1373K, the amount of HfB₂ increases as it is evident from Table-2.

Referring back to Table-1, we find that the same HfB species is present and this is a major component among the Hf species in the Hf-doped MgB₂ sample annealed at 1173K. On the other hand, HfB₂ is a minority phase at this temperature. There are two more sites where Hf resides which correspond to the remaining two frequencies ($\omega_Q=59.5$ Mrad/s and 248.9 Mrad/s). It is highly probable that Hf can go to both Mg and B sites, which gives rise to these two frequencies. The justification for this assumption stems from V_{zz} of these two lattice sites. Literature data on the EFG [22,23] from an NMR study at these two sites using ²⁵Mg and ¹²B, respectively, showed that the EFG at the B site is nearly five times larger than that at the Mg site. Our results presented in Table-2 also have a similar ratio (>4.0). However, the absolute values of the EFG for ¹⁸¹Ta probes compared to other probes [24] are high and hence the same trend is expected for Mg or B sites. A logical conclusion would be that Hf occupies both Mg and B positions. The site occupancies of the two sites are not simply statistical but a consequence of the chemical potential between Ta and the surrounding atoms. However, considering the

ionic radii of the species involved (Mg(2+), Hf(4+), and B(-1) being 0.074, 0.071 and 0.09nm, respectively), it is highly probable that Hf predominantly occupies the Mg site. Moreover, from the results of T_c (in particular $T_c^{(\text{onset})}$) it is obvious that Hf occupies B site to a less extent than Mg site. Thus the TDPAC results mentioned in Table-1 clearly indicate that the site-II corresponds to Mg and site-III to B. Considering the site occupancy it is quite obvious that the largest component HfB may precipitate and act as the most effective pinning centre for the enhancement of J_c . The other two substitutions, i.e. Hf in Mg and B sites play minor roles in the enhancement of H_{c2} .

Conclusion:

We have observed a considerable enhancement of J_c , H_{irr} and also H_{c2} in 1% Hf-doped MgB_2 , contrary to charged particle irradiation. There was little change in $T_c^{(\text{onset})}$ rendering Hf-doping an effective means to enhance J_c without losing superconducting properties. The enhancement of J_c is caused primarily by HfB and HfB_2 precipitations at grain boundary, whereas the increase of H_{c2} points towards substitution of Hf at B and Mg sites. Substitution at B site would affect 2D σ -bands and hence $T_c^{(\text{onset})}$, whereas that at Mg site would affect the 3D π -bands and hence increase the resistivity. The insignificant change of $T_c^{(\text{onset})}$ points towards Hf occupying Mg site dominantly. There has been a considerable increase in resistivity as well as the transition width, implying a reduction of grain connectivity, too. The TDPAC spectra of Hf-doped MgB_2 revealed four inequivalent sites which were compared with the reference Hf-boride annealed at the temperature of formation of MgB_2 and at a higher temperature. From XRD it is evident that at the temperature of formation of MgB_2 , the major species formed is HfB, which was converted to the thermodynamically stable phase HfB_2 at higher

temperatures. Thus, HfB precipitates formed in Hf-doped MgB₂ act as effective pinning centres for the enhancement of J_c, the grain boundary pinning mechanism being dominant. There is an indication of partial occupation of both Mg and B sites by Hf as evident from the relative EFG of other two components. At 1% doping, this partial occupation of B site if at all, does not destroy the superconductivity. Higher levels of doping may be attempted to investigate the occupancy of Hf at B site and its effects. But the 1% level of Hf-doping is beneficial from the point of view of superconductivity. We are planning to carry out the synthesis of Hf-doped MgB₂ at temperatures higher than 1173 K and observe J_c to further elucidate the role of HfB/HfB₂ for the enhancement of J_c.

Acknowledgement:

Authors sincerely thank Dr. S.V. Thakare, Radiopharmaceuticals Division, BARC, Dr. Ms. P. Mukherjee, Material Group, VECC and Dr. K. Krishnan, Fuel Chemistry Division, BARC for their help in the experiment. They are also thankful to Dr. V.K. Manchanda, Head Radiochemistry Division, BARC and Dr. S.K. Aggarwal, Head, Fuel Chemistry Division, BARC for their keen interest in this work. One of the authors (AT) thanks CSIR for the research grant.

References:

1. A.Talapatra, S.K.Bandyopadhyay, Pintu Sen, A.Banerjee and R. Rawat, *Superconductor Science and Technology* 20 (2007) 1193.
2. N. Horhager, M. Eisterer, H.W. Weber, T. Prikhna, T. Tajima and V.F. Nesterenko, *J. of Physics: Conf. Series* 43 (2006) 500.
3. R.J.Cava, H.Zandberger and K.Inumaru, *Physica C* 385 (2003) 8.
4. A. Talapatra, S. K. Bandyopadhyay, Pintu Sen, A. Sarkar and P Barat, *Bull. Mater. Sci.* 27, (2004) 429.
5. T. Butz, S. Saibene, T. Fraenzke and M. Weber, *Nucl. Inst. Met. A* 284 (1989) 417.
6. S. Haigh, P. Kovac, T.A. Prikhna, Ya. M. Savchuk, M.R. Kilbum, C.Salter, J. Hutchison and C. Grovener, *Supercond. Sci.Technol.* 18 (2005) 1190.
7. A. Matsumoto, H. Kumakura, H. Hkitaguchi, B.J. Sencowicz, M.C. Jewell, E.E. Hellstrom, Y. Zhu, P.M. Voyles and D.C. Larbalestier, *Appl. Phys. Lett.* 89 (2006) 132508.
8. S.K. Chen, M. Wei and MacManus-Driscoll, *Appl. Phys. Lett.* 88 (2006) 192512.
9. O. Perner, W. Hablar, J. Eckert, C. Fisher, C. Mickel, G. Fuchs, B. Holxapfel and L. Schultz, *Physica C* 432 (2005) 15.
10. O.de la Pena, A. Aguuayo and R. de Coss *Phys. Rev. B* 66 (2002) 012511.
11. J. Kortus, I.I. Mazin, K.D. Belashchenko, V.P. Antropov and I.I. Baayer, *Phys. Rev. Lett.* 86 (2001) 4656.
12. V. Braccini, A.Gurevich, J. E. Giencke, M. C. Jewell, C. B. Eom, D. C. Larbalestier, A. Pogrebnyakov, Y. Cui, B. T. Liu, Y. F. Hu, J. M. Redwing, Qi Li, X. X. Xi, R. K. Singh, R. Gandikota, J. Kim, B. Wilkens, N. Newman, J. Rowell, B. Moeckly, V.

Ferrando, C. Tarantini, D. Marré, M. Putti, C. Ferdeghini, R. Vaglio, and E. Haanappel-
Phys. Rev. B 71 (2005) 012504.

13. V. Ferrando, P. Manfrinetti, D. Marre, M. Putti, I. Sheikin, C. Tarantini and C.
Ferdeghini, Phys. Rev. B 68 (2003) 49.

14. I.I. Mazin and V.P. Antropov, Physica C 385 (2003) 49.

15. J.M. Rowell, Supercond. Sci. Technology, 16 (2003) 17.

16. S.X. Dou, S. Soltanian, J. Horvat, X.L. Wang, S.H. Zhou, M. Ionesu and H.K. Liu,
Appl. Phys. Lett. 81 (2002) 3419.

17. A. Gurevich, S. Patnaik, V. Braccini, K.H. Kim, C. Mielka, X. Song, L.D. Cooley,
S.D. Bu, D.M. Kim, J.H. Choi, L.J. Belenky, J. Giencke, M.K. Lee, W. Tian, X.Q. Pan,
A. Siri, E.E. Hellstrom, C.B. Eom and D.C. Larbalestier, Supercond. Sci. Technol. 17
(2004) 278.

18. A. Yamamoto, J. Shimoyama, S. Vada, Y. Katsura, I. Iwayama, S. Horii and K.
Kishio, Appl. Phys. Lett. 86 (2005) 212502.

19. O. Mura, H. Tomioka, D. Ito and H. Narada, JI. of Phys. 97 (2008) 012156.

20. T. Butz, Hyperfine Interactions 52 (1989) 189.

21. E.N. Kaufmann, J. Phys. Chem. Solids, 34 (1973) 2025.

22. Sylvio Indris, Paul Heitjans, Jens Hattendorf, Wolf-Dietrich Zeitz and Thomas
Bredow, Phys. Rev. B 75 (2007) 024502.

23. M. Mali, J. Roos, A. Shengelaya, H. Keller and K. Conder, Phys. Rev. B
65(2002)100518(R)

24. Seung-back Ryu, Satyendra Kumar Das, Tilman Butz, Werner Scmitz, Christian
Spiel, Peter Blaha, Karlheinz Schwaez, Phys. Rev. B 77, 094124 (2008).

Table1. TDPAC parameters: quadrupole frequency ω_Q ,
 asymmetry parameter η , Lorentzian frequency distribution δ ,
 and site occupancy for ^{181}Hf in MgB_2

Annealing temp: 1173K

Site	ω_Q (Mrad/s)	η	δ (%)	Site %
I	32.3(5)	0.41(2)	8.2 (5)	49
II	59.5(9)	0.17(6)	12.1(1.7)	26
III	248.9(7)	0.17(5)	8.0(1)	16
IV	112.7(5)	0.10(1)	1.9(7)	9

Table 2. TDPAC parameters: quadrupole frequency ω_Q , asymmetry parameter η ,
 Lorentzian frequency distribution δ , and site occupancy for ^{181}Hf in HfB_x

Site	ω_Q (Mrad/s)	η	δ (%)	Site %
Annealing Temperature 1173K				
I	34.1(2)	0.45(4)	8.2(3)	34
II	113.2(4)	0.1(1)	2.4(4)	66
Annealing Temperature 1373K				
I	34.0(2)	0.41(6)	2.6(4)	10
II	113.3(1)	0.10(1)	0.3(1)	90

Figure Captions:

Fig. 1 XRD patterns of (a) Hf-doped MgB_2 , (b) HfB_2 annealed at 1173K

Fig. 2. Resistivity versus temperature for pristine MgB_2 and Hf-doped MgB_2 . Inset shows superconducting transitions for the samples to indicate the transition width.

Fig. 3. Upper critical field (H_{c2}) of undoped and Hf-doped MgB_2 . Inset shows irreversibility field line $H_{irr}(T)$ of the samples. The behaviour of H_{c2} and H_{irr} is similar.

Fig. 4. Critical current density of undoped and Hf-doped MgB_2 at (a) 2 K and (b) 20 K.

Fig. 5. Pinning force density at various temperatures of undoped and Hf-doped MgB_2 .

Fig. 6. TDPAC spectrum (left) and cosine-transform (right) of Hf-doped MgB_2 annealed at 1173 K. The points correspond to the experimental data and line to the fit of the experimental data.

Fig. 7. Top: TDPAC spectrum (left) and cosine-transform (right) of HfB_x annealed at 1173 K.

Bottom: annealed at 1373 K. The points correspond to the experimental data and line to the fit of the experimental data.

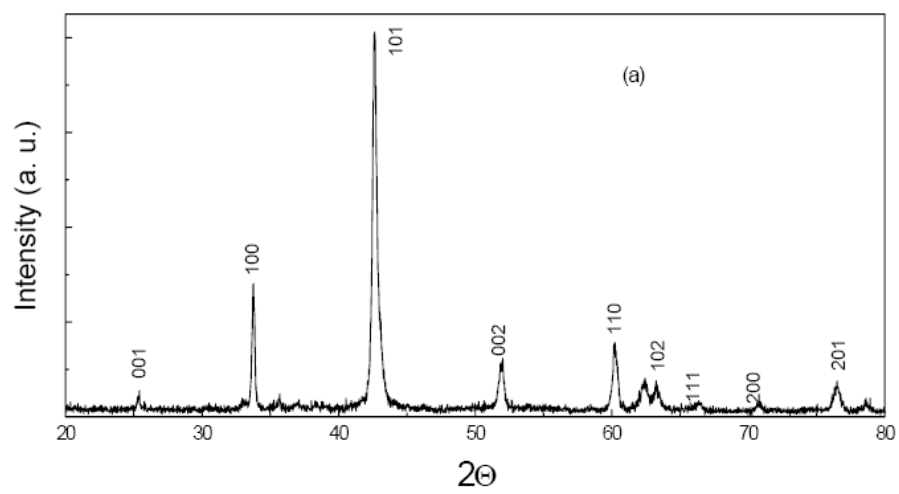


Fig 1 (a)

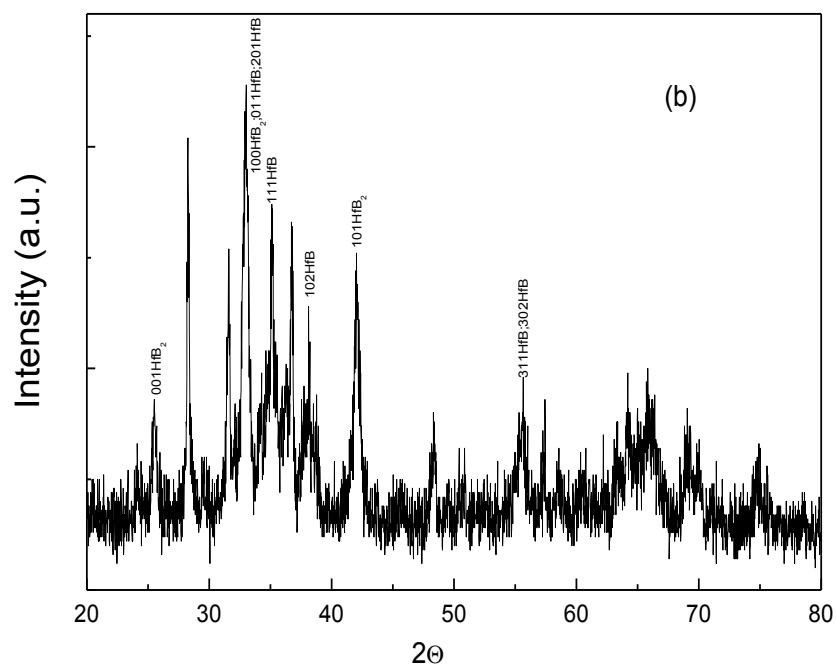


Fig 1 (b)

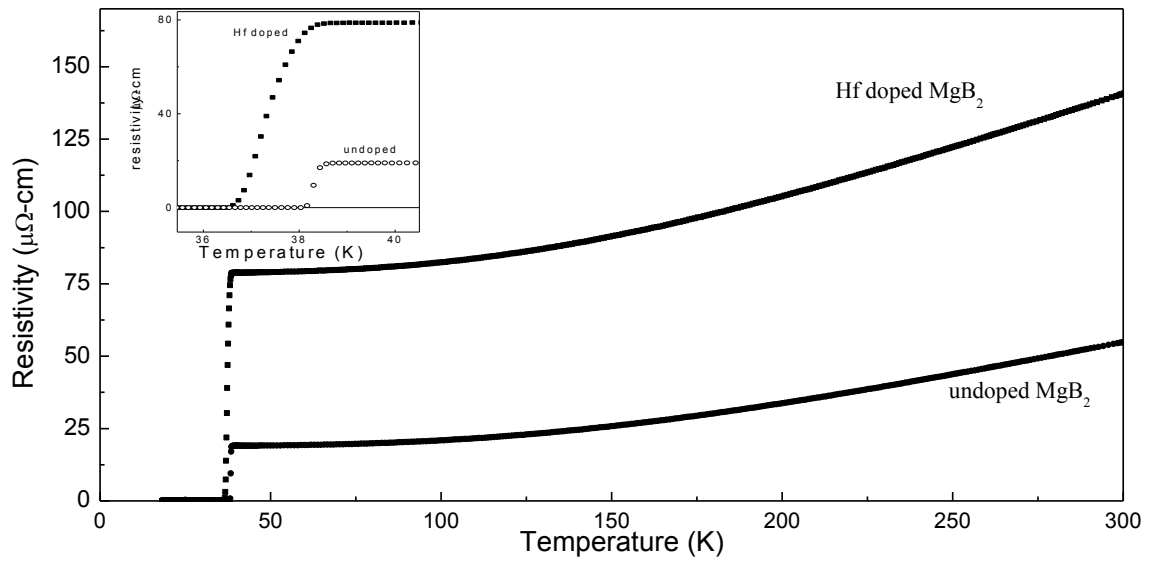


Fig. 2

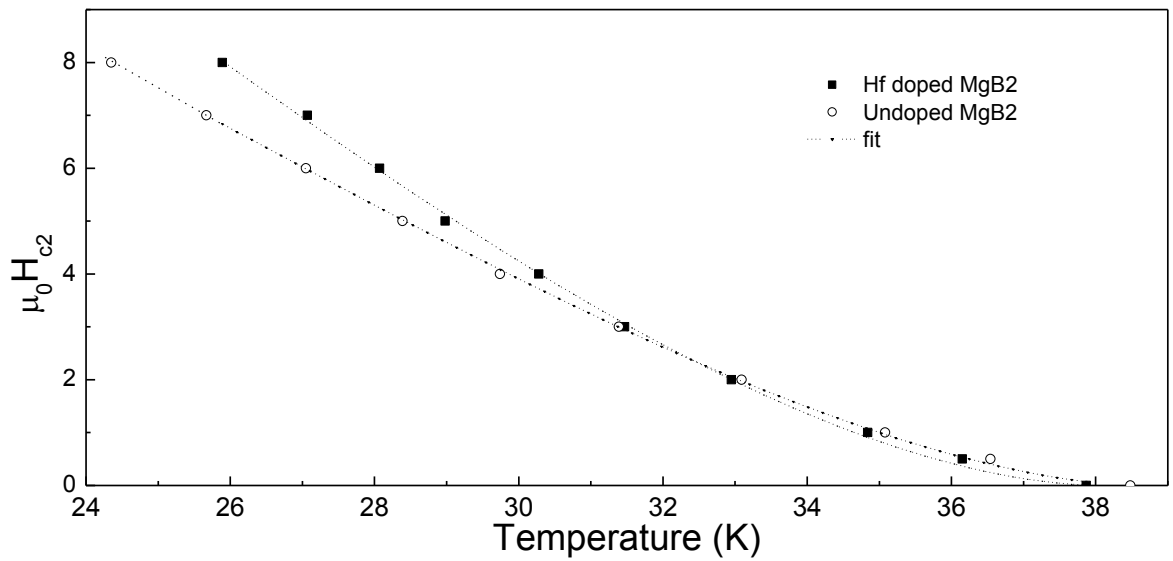


Fig. 3

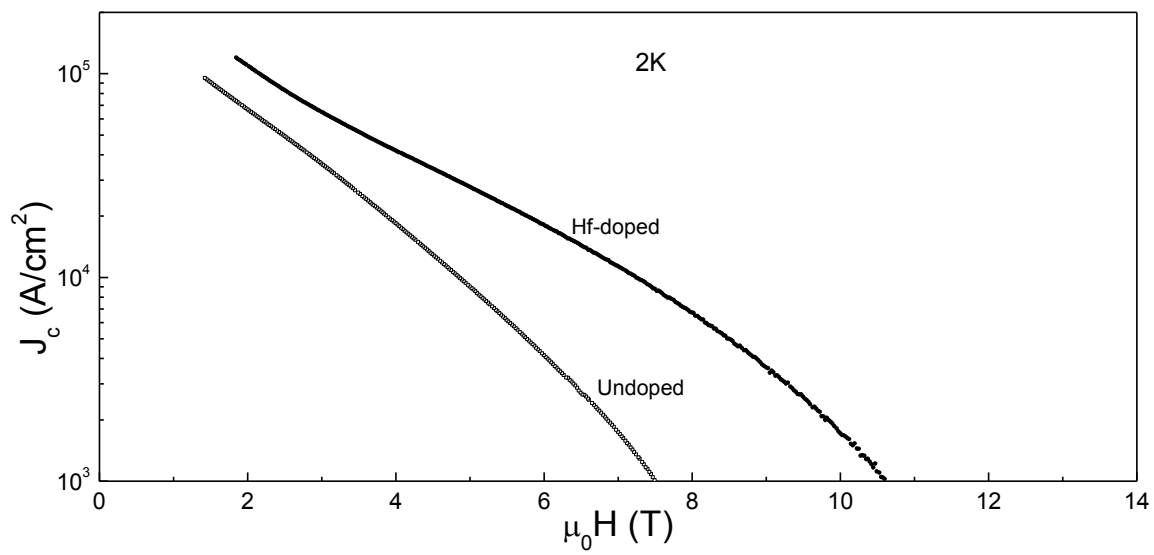


Fig. 4a

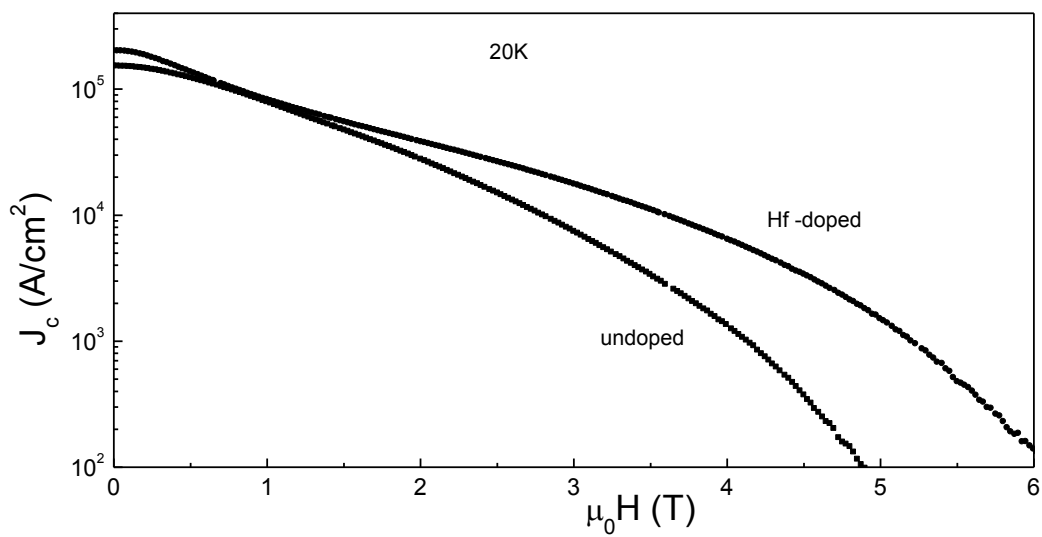


Fig 4 (b)

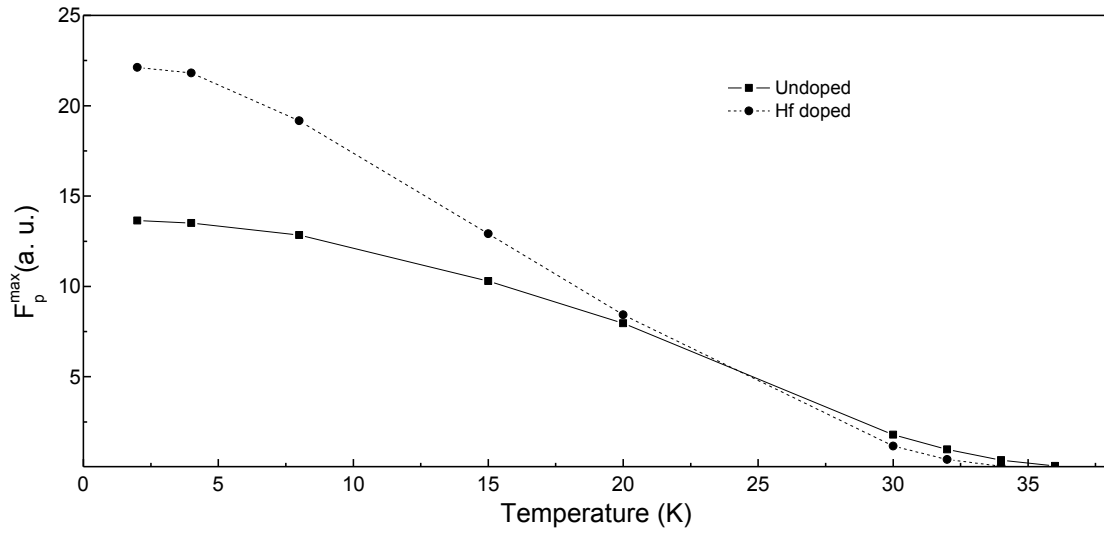


Fig. 5

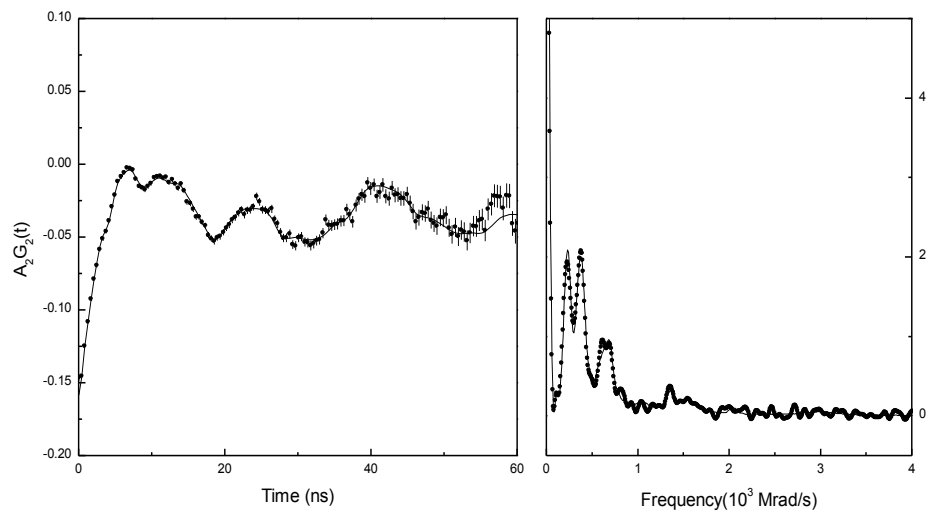


Fig 6.

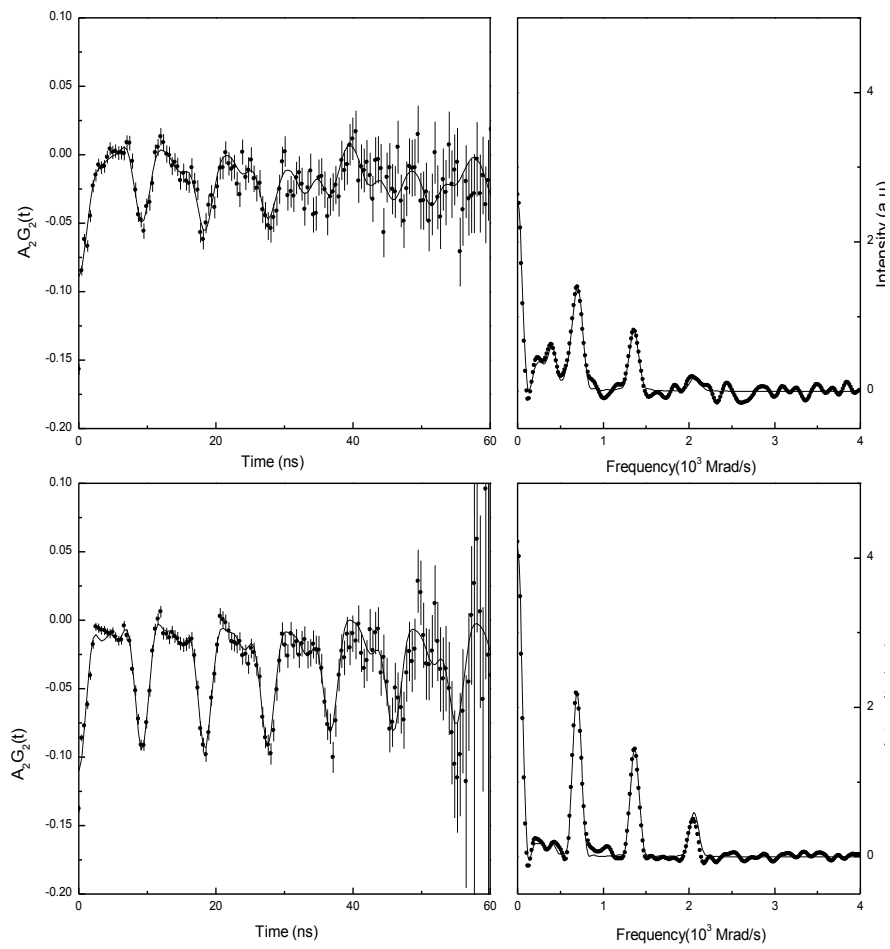


Fig 7.